Retroactivity Controls the Temporal Dynamics of Gene Transcription

Shridhar Jayanthi, Kayzad S. Nilgiriwala and Domitilla Del Vecchio

February 8, 2013

Abstract

Just like in many engineering systems, impedance-like effects, called retroactivity, arise at the interconnection of biomolecular circuits, leading to unexpected changes in a circuit's behavior. In this paper, we provide a combined experimental and theoretical study to characterize the effects of retroactivity on the temporal dynamics of a gene transcription module *in vivo*. The response of the module to an inducer was measured both in isolation and when the module was connected to downstream clients. The connected module, when compared to the isolated module, responded selectively to the introduction of the inducer versus its withdrawal. Specifically, a "sign-sensitive delay" appeared, in which the connected module displayed a time delay in the response to induction and anticipation in the response to de-induction. The extent of these effects can be made larger by increasing the amounts of downstream clients and/or their binding affinity to the output protein of the module. Our experiment results and mathematical formulas allow to predict the extent of the change in the dynamic behavior of a module after interconnection. They can be employed to both recover the predictive power of a modular approach to understand systems or as an additional design tool to shape the temporal behavior of gene transcription.

1 Introduction

The temporal dynamics of gene transcription control a number of important cellular processes, such as responding to environmental changes, reaching adaptation to external perturbations, and executing the cell cycle and circadian rhythms.[1] Recent experimental evidence shows that cell fate is determined on the basis of the temporal dynamics of competing gene programs,[2] suggesting that temporal dynamics ultimately controls a cell's phenotype. In synthetic biology, the precise control of the dynamics of gene transcription has been instrumental for designing a number of clocks[3–5] and incoherent feedforward loops to reach adaptation.[6] Understanding the mechanisms that control temporal dynamics in gene transcription is also necessary to determine the extent of modularity in biomolecular circuits. In fact, it is well known that the dynamic behavior of a system may not be modular even when its static behavior is.[7]

Biomolecular networks are composed of recurrent structural modules such as transcription components in gene networks and covalent modification cycles in signal transduction networks. A fundamental question is whether these structural modules preserve their behavior whether they are connected to each other or they are in isolation. In addition to having deep implications from an evolutionary perspective,[8] modularity allows to predict the behavior of a complex network by simply composing the behavior of its subsystems characterized in isolation.[9–11] Hence, modularity simplifies the problem of understanding the functionality of complex natural systems and allows to design synthetic biology circuits through a bottom-up approach.

Previous theoretical studies, however, suggested that the dynamic behavior of a module characterized in isolation changes upon interconnection with other modules due to loading effects, which were called retroactivity to extend the notion of impedance to non-electrical systems.[12–14] Retroactivity is the phenomenon by which a downstream system changes the

dynamic state of an upstream system in the process of receiving information from the latter (Figure 1) and it is related to the concept of fan-out in digital electronics.[15] Consider the connection between two systems illustrated in Figure 1. By design, we expect the information to travel from the "upstream" to the "downstream" system. However, when a downstream system receives (observes) information from an upstream system, exchange of "matter" must necessarily take place between the two systems. This exchange of matter, in turn, changes the state of the upstream system. For example, to measure the pressure of a tire (upstream system) we need to connect it to a measurement device (downstream system). But, in doing so, some air will flow between the two systems affecting the tire pressure. While measurement devices have been designed on purpose to minimize retroactivity, biomolecular circuits may not minimize it and may actually use it in advantageous ways.

As an example, consider an activator-repressor clock[3] whose signaling elements are transcription factors, an activator and a repressor protein. Suppose that the clock is "connected" to a downstream system, such as a reporter, so that a protein in the clock regulates the expression of the reporter. The biochemical interaction that allows this regulation is the binding of the protein to operators in the reporter. When this binding occurs, the clock protein is not available anymore for the reactions that make the clock, leading to a change in the clock behavior. It has been theoretically shown that this phenomenon can disrupt the clock if the protein used for connection is the activator while it can enhance the clock performance if the protein used is the repressor.[16] Hence, it has been argued that retroac-

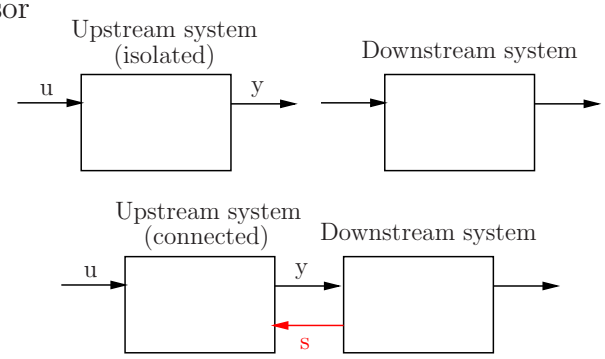

Figure 1: **Retroactivity** is the unavoidable back-action (indicated by the red arrow s) from a downstream system to an upstream system. It is due to the fact that the downstream system, in order to receive the information in y, uses up some of y. Hence, y cannot fully take part to the network of interactions that constitutes the upstream system, resulting in a change of the upstream system behavior.

tivity may be among the possible reasons of unpredictable behavior of composed synthetic circuits.[17] Characterizing retroactivity effects in a systematic way is thus necessary to recover predictable power when composing systems in a bottom-up fashion.

A few experimental studies have recently appeared on retroactivity in various types of biological networks both *in vitro* and *in vivo*.[18–22] Of particular relevance to this paper are those considering dynamic behavior. Specifically, the effect of retroactivity from DNA load on a synthetic transcription clock was studied through cell-free experiments *in vitro*, which showed a detrimental effect on the clock behavior from the downstream load.[22] Further *in vitro* experimental studies focused on retroactivity in signal transduction cascades. These studies showed that retroactivity alters the temporal dynamics of a covalent modification cycle by substantially decreasing the frequency bandwidth.[21]

In this paper, we perform a combined theoretical and experimental study to systematically characterize the effects of retroactivity from downstream clients on the temporal dynamics of a gene transcription module in *vivo*.

2 Results and Discussion

2.1 Gene circuit to study retroactivity

Figure 2(a) shows the details of the gene circuit employed to characterize retroactivity effects. The upstream transcription component takes as input atc (u) and provides as an output LacI-LVA (y). LacI is in turn taken as an input by a reporter system assembled on the same plasmid as the transcription component. The reporter system produces GFP-LVA as an indirect measurement of LacI. Since LacI is a repressor, we should expect that GFP decreases as atc increases. The downstream clients contain LacI operators and are assembled on a different plasmid. Both the reporter and the downstream clients apply retroactivity to the upstream transcription component (see Figure 2(b)). Retroactivity from LacI binding

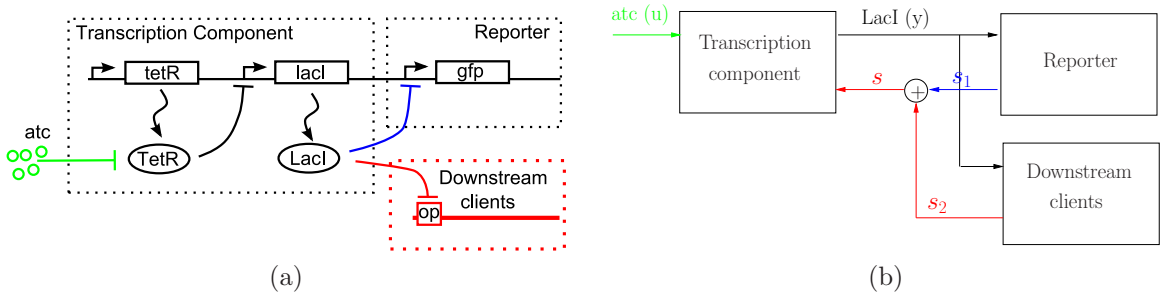

(a) (b)

Figure 2: **Layout of gene circuit employed to study retroactivity.** (a) Genetic diagram. The circuit plasmid contains both the transcription component and the reporter system. The downstream clients to which the transcription component connects are realized by a plasmid containing one operator site with affinity to LacI. The *connected system* refers to cells co-transformed with both the circuit plasmid and the plasmid with operator sites. The *isolated system* refers to cells co-transformed with the circuit plasmid and a plasmid that does not contain the operator site but is of the same type as the one with operator site. (b) Block diagram illustration of the different parts of the gene circuit. The transcription component takes as input u anhydrotetracycline (atc) and gives as output y the repressor LacI. This output is used as an input by both the reporter system and the downstream clients. Upon interconnection with either the reporter or the downstream clients, retroactivities s_1 from the reporter and s_2 from the downstream clients, respectively, arise.

sites present in the bacterial genome were not included in the model since the genome relative concentration is insignificant compared to the concentration of plasmids in the cell, as discussed in the Materials and Methods section. Here, we are interested in characterizing the effects of retroactivity s_2 from the downstream clients on the response of the transcription component to atc. Hence, we consider as the *isolated system* the circuit of Figure 2(a), in which the operator sites in the downstream clients are absent, resulting into $s_2 = 0$. We consider as the *connected system* the circuit of Figure 2(a), in which the operator sites in the downstream clients are present.

Experimentally, we realize the isolated system through cells in which we co-transformed the pACYC184-based plasmid (with the transcription component and reporter), which we refer to as circuit plasmid, with pUC18-based plasmid that does not have LacI operator sites, which we refer to as blank plasmid. We realize the connected system through cells in which we co-transformed the circuit plasmid with pUC18-based plasmid including the operator site for LacI, which we refer to as client plasmid. The difference between the

responses of GFP to atc in the isolated and connected system configurations characterize the effects of retroactivity s_2 from the downstream clients on the transcription component. These experiments were performed in *E. coli* strain KL-323, chosen due to its mutations in its *lacI* and *recA* genes. Its genome also contains the LacZ promoter, which has affinity to LacI. However, due to its little relative concentration, the retroactivity from genome can be neglected.

We modeled the circuit of Figure 2(a) by a set of ordinary differential equations (ODE) describing the rate of change of LacI and GFP. Let p_T be the concentration of the circuit plasmid (proportional to the circuit plasmid copy number) and q_T be the concentration of the clients plasmid (proportional to the clients plasmid copy number). Let $\lambda = q_T/p_T$, $l = [LacI]/p_T$, $g = [GFP]/p_T$, let c_1 denote the concentration of LacI bound to downstream clients promoter sites divided by p_T, and let c_2 denote the concentration of LacI bound to the promoter of the reporter divided by p_T. Then, we have the following ODE model for the connected system:

$$\begin{aligned}
\dot{l} =& \alpha_1 \frac{u^n}{1+u^n} - \delta l \overbrace{\underbrace{-(p_T k'_{\text{on}})l(1-c_1) + k'_{\text{off}}c_1}_{s_1} \underbrace{-(p_T k_{\text{on}})l(\lambda - c_2) + k_{\text{off}}c_2}_{s_2}}^{s} \\
\dot{c}_1 =& (p_T k'_{\text{on}})l(1-c_1) - k'_{\text{off}}c_1 - \delta c_1 \\
\dot{c}_2 =& (p_T k_{\text{on}})l(\lambda - c_2) - k_{\text{off}}c_2 - \delta c_2 \\
\dot{g} =& \alpha_2(1-c_1) - \delta g,
\end{aligned} \tag{1}$$

in which u is the concentration of atc in units of its dissociation constant from TetR, n is the cooperativity of atc binding TetR, $k_{\text{on}}, k'_{\text{on}}, k_{\text{off}}, k'_{\text{off}}$ are the association and dissociation rate constants, respectively, of LacI with the promoter and operator sites, and δ is the decay rate constant (including dilution and degradation). Here, α_1 and α_2 are the maximal expression rates per promoter. Since the complexes also decay, we are assuming the non-asylum model

according to which proteins are not protected by decay when bound to DNA.[23] The reader is referred to the SI for the detailed derivation of the model and for the parameter values.

Note that the retroactivity term s_2 depends only on λ and not on the absolute value of the downstream clients amount q_T. This indicates that the effects of retroactivity depend on the ratio between the circuit plasmid copy number and the clients plasmid copy number, but not on the absolute value of the latter. We remark that the binding/unbinding reactions are much faster than the production and decay of LacI. Furthermore, the dissociation constant $K_{\mathrm{d}} = k_{\mathrm{off}}/(p_T k_{\mathrm{on}})$ of LacI with the operator sites is very small, implying that once LacI binds, it unbinds very rarely. These features are relevant for understanding the experimental results illustrated in the following section.

The retroactivity to the output of the transcription component s appears as a rate in the equation for LacI and has two components: s_1 is the retroactivity due to the reporter and s_2 is the retroactivity due to the downstream clients. Here, we study the effect that s_2 has on the response of LacI to atc, indirectly measured through GFP. Hence, the isolated system is represented by the above equations, in which we have set $s_2 = 0$, but $s_1 \neq 0$. It follows that the isolated system configuration still has an intrinsic retroactivity due to the reporter. Given that the expressions of s_1 and s_2 are similar, the qualitative effects that s_1 has on the transcription component are the same as those that s_2 has. Therefore, to characterize the qualitative effect of retroactivity s on the transcription component, it is enough to characterize the effect of s_2 on the response of GFP to atc.

2.2 Effects of retroactivity on the response of the gene circuit

We characterize the effects of retroactivity on the dynamic response of GFP to sudden changes of atc. For completeness, we also show the effects on the steady state transfer curve from atc to GFP. For the dynamic response, we consider two experiments: an induction experiment and a de-induction experiment. In the induction experiment, LacI starts from

zero (GFP starts from its maximal unrepressed value) at time zero and a high constant non-zero value of atc is applied, so that LacI rises and GFP decreases reaching zero. In the de-induction experiment, LacI starts from a non-zero steady state reached through pre-induction with a non-zero high value of atc (so that GFP starts from zero). Then, atc is suddenly removed ($atc = 0$) so that LacI decreases toward zero and GFP rises toward its maximal unrepressed value. This characterization was performed at the population level, by measuring cultures growing in a plate reader, and at the single cell level, by imaging microcultures in a microscope. In order to quantify the effect of retroactivity on dynamics, we measure the response time of GFP, which mirrors the one of LacI. There are several standard metrics to determine the response time of a system. In this paper, we consider the t_{50}, which is given by the time the fluorescence changes by 50% and t_{20} which is given by the time the fluorescence changes by 20% of its maximal unrepressed value from when atc is applied or removed.

Dynamic effects of retroactivity: Induction. Figure 3(a) shows a simulation and Figure 3(b) shows a representative response of GFP to sudden application of atc for both the isolated and connected systems as measured in a plate reader. The effect of retroactivity is basically a time delay. This can be qualitatively explained by recalling that the value of the dissociation constant K_{d} for LacI binding to its operator sites is extremely small and that the binding reactions are much faster that protein production and decay (see the SI for the exact values). In fact, LacI is sequestered by the operator sites as soon as it is produced. Only when the operator sites are filled, any additional LacI produced is free to take part in other reactions, and, in particular, in those of the reporter. Hence, before LacI can rise (GFP can decrease), there is a time delay, which is the time it takes for LacI to fill the operator sites. This time delay, monotonically increases with the relative amount λ of these sites. The reader is referred to next section for a precise mathematical explanation.

Figure 3(c) shows the response times for isolated and connected systems. The response

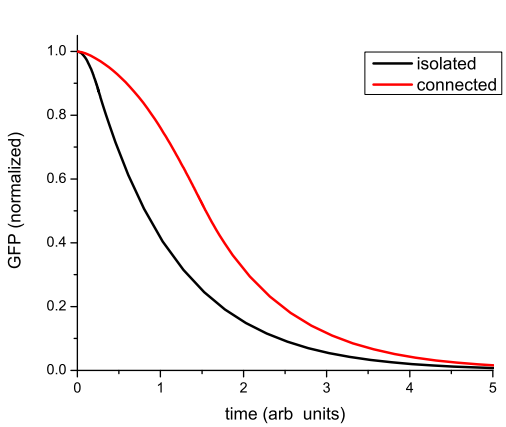

(a) Simulation.

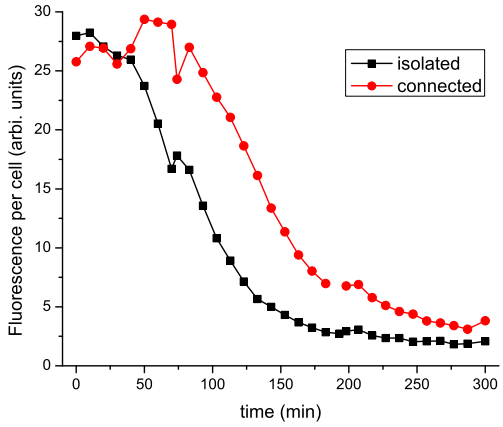

(b) Experiment.

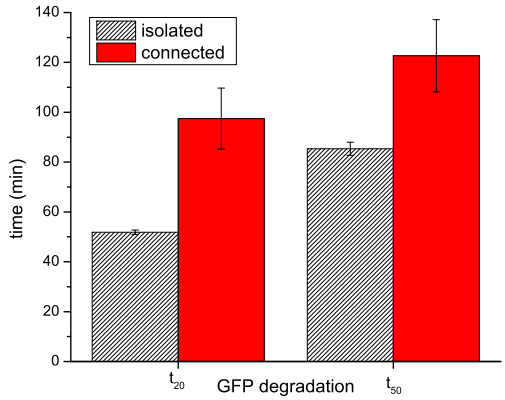

(c) Mean response times (0.095 μM atc).

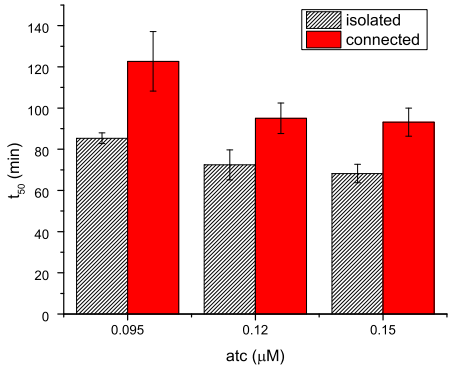

(d) t_{50} increasing atc.

Figure 3: **Retroactivity delays the response to sudden input stimulation.** (a) Simulations from the model in equations (1). The units in this simulation are nondimensionalized. Parameters used in this simulation are given in the SI. (b) Data from population measurements in plate reader show good agreement with the model. This plot shows a representative time course for the induction experiment with 0.095μM atc. (c) Response times to induction with 0.095 μM atc. The average half-life of GFP (t_{50}) post-induction increased by 43%, going from 85±2min to 122±16min. The slow response occurs mainly in the early stages of induction and can be quantified by calculating the t_{20}, the time it takes to remove 20% of the GFP. The t_{20} presents an average delay of 40min, slightly higher than the 37min delay in the half-life value (t_{50}). (d) Higher levels of atc can decrease the t_{50}, but the delay caused by retroactivity persists. In both (c) and (d), averages were calculated from three different experiments. Error bars denote one standard deviation around the average. More data is given in the SI. Data displayed in (b)-(d) was obtained from plate reader measurements.

time of the connected system increases in average by 40% with respect to the one of the isolated system. The minimal and maximal increases are of 24% and of 64%, respectively. Figure 3(d) shows that increasing the amount of atc, the response times for both isolated and connected systems decrease. However, the delay caused by retroactivity persists. This implies that the dynamic effect of retroactivity cannot be removed nor attenuated by choosing higher input values, that is, it cannot be pre-compensated. Thus, in order to keep the speed of response of the output in the connected system close to the one of the isolated system, feedback control is required. Through feedback control, one can design circuits that are effectively insulated from retroactivity and behave the same whether connected or isolated.[12,24]

Dynamic effects of retroactivity: De-induction. Figure 4 shows the response of GFP to sudden removal of atc for both the isolated and connected systems, as measured in a plate reader. Surprisingly, the connected system responds faster (by about 50min) than the isolated system when atc is suddenly removed. This apparently counter-intuitive result can be explained as follows. In the isolated system, the only mechanism by which free LacI can be removed is through dilution and/or degradation. In the connected system there is an additional mechanism by which LacI can be removed. Since the complex C_2 of LacI bound to operator sites also dilutes but the operator sites do not dilute or degrade, free LacI can be removed by binding to the operator sites. The continuous dilution of LacI in complexes C_2 guarantee the presence of free operator sites during the de-induction, which can in turn bind to more free LacI. If the operator sites were protecting LacI from degradation and the system had no dilution (no growth), we should have observed a slower response in the connected system just like in the induction experiment. The reader is referred to the next section for a mathematical explanation of this phenomenon and to the SI for the mathematical derivations.

Hence, because of retroactivity a sign-sensitive delay arises: when the input stimulation

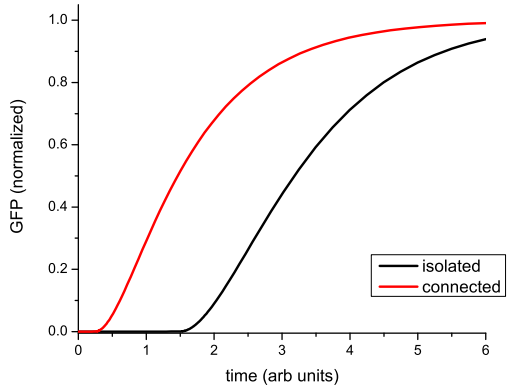

(a) Simulation.

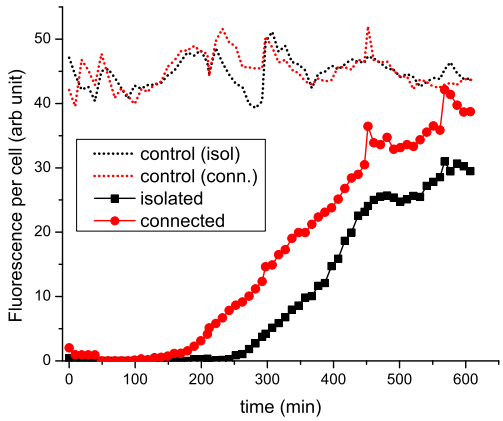

(b) Experiment.

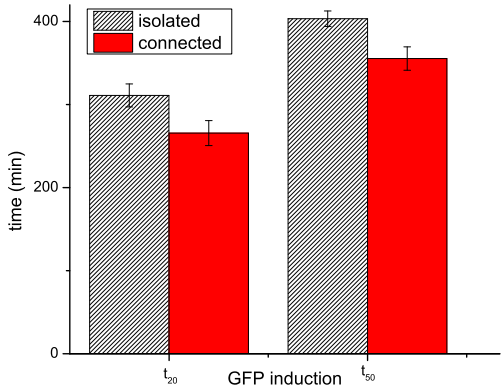

(c) Mean response times.

Figure 4: **Retroactivity speeds up the response to sudden removal of input stimulation.** (a) Simulation of the model in equation (1) illustrates the effect of retroactivity on the response to removal of atc. The atc input is removed at time zero. (b) Data from population measurements in plate reader validate the model prediction. This plot shows a representative time course of the de-induction experiment. The connected system shows an anticipation, with respect to the isolated system, of about 50min in the response to removal of inducer from cultures pre-induced with .15μM atc for 400min. Specifically, the average t_{50} from six experiments went down from 403$\pm$7min in the isolated system to 355$\pm$12min in the connected system. The dotted lines show the maximal unrepressed steady state values of GFP for connected and isolated systems. (c) The increase in the speed of response occurs mainly in the early stages, indicating a time delay between the connected and isolated systems. In (c), average was calculated from six samples. Error bars denote one standard deviation around average. Data in (b)-(c) was obtained from plate reader measurements.

is suddenly applied, the connected system presents a delay of about 40%. By contrast, when the input stimulation is suddenly removed, the connected system presents an anticipation of the response of about 50min.

Retroactivity impact at the single cell level. Effects observed in population assays may be different from effects at the single cell level.[25] Figure 5 shows the effect of retroactivity on the dynamic response in microcolonies of isolated and connected systems undergoing atc induction and de-induction. The measured half-life post induction with 0.125μM atc went from 53 ± 5min in the isolated system to 75$\pm$10min in the connected system (interval denotes one standard deviation around average across six microcolonies). For the de-induction experiment, the response time was calculated with the assumption that steady-state was reached at 300min. The time until the microcolonies reached 50% of the steady-state went from 191 ± 35min in the isolated system to 99 ± 26min in the connected system (interval denotes one standard deviation around average across two microcolonies). These results are consistent with those obtained from population measurements in the plate reader. Additional data and details can be found in the Supplementary Information.

Effects of retroactivity on the steady state transfer curve. To obtain the steady state transfer curve, we performed a series of experiments in which the steady state value of GFP was recorded in response to different constant values of atc (see the SI for the full time traces). This is shown in Figure 6. The shape of the transfer curve is well characterized by the point of half maximal induction, called u_{50}, and by the apparent Hill coefficient n_H. The u_{50} corresponds to the value of the input stimulation for which the output response is 50% of the maximal. As seen in Figure 6, the experimental data showed an increase of about 30% in the u_{50}, going from 0.054$\pm$0.001μM in the isolated system to 0.069$\pm$0.01μM in the connected system (standard error). There was no significant change in the apparent Hill coefficient n_H (9.7$\pm$1.3 for the isolated system and 9.1$\pm$1.5 for the connected system, standard error). When the input stimulation atc increases, LacI is produced but it is immediately sequestered

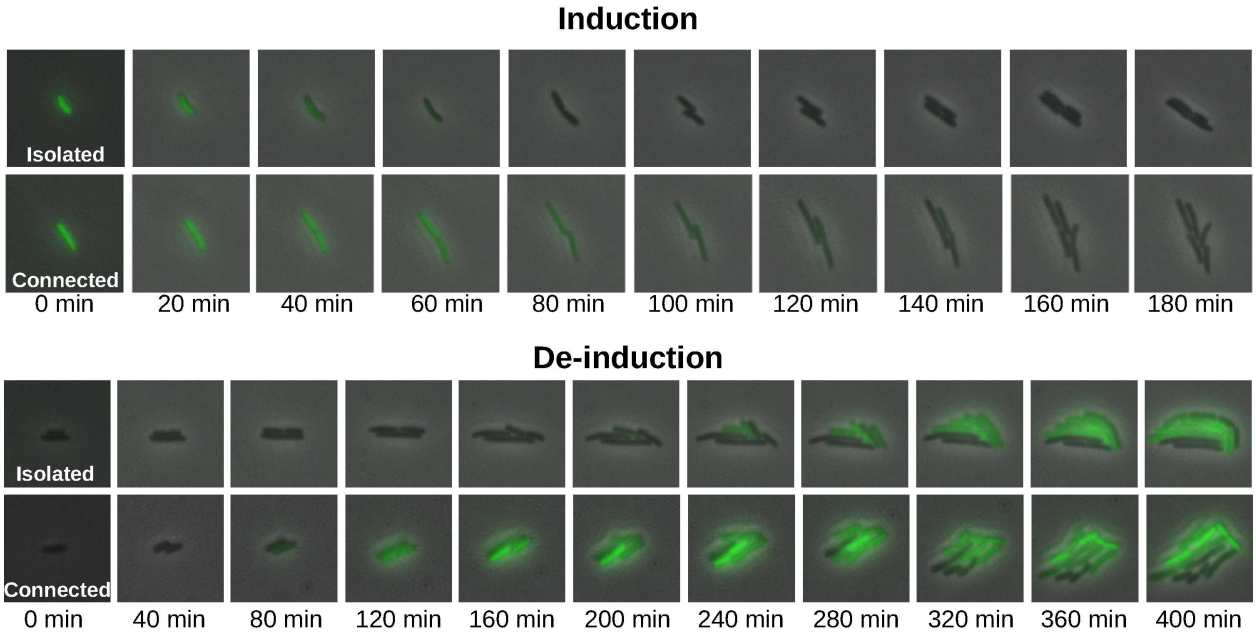

(a) Induction and de-induction in the microscope.

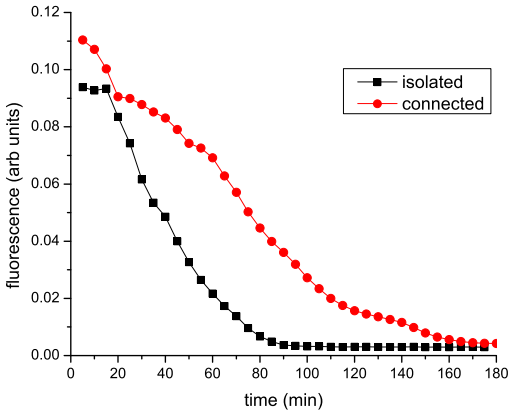

(b) Quantification of induction assays.

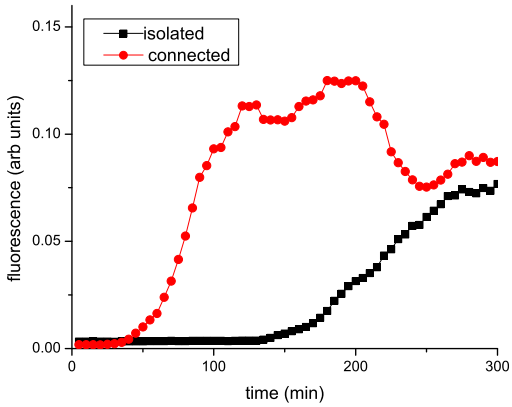

(c) Quantification of de-induction assays.

Figure 5: **Effects of retroactivity at the single cell level.** (a) The sequence of images illustrates the response of microcolonies of isolated and connected systems to addition and removal of 0.125 μM atc. As with the population experiments in plate reader, the connected system response is slower during an induction and faster during a de-induction when compared to the isolated system. (b)-(c) Quantification of the representative microcolonies to induction and de-induction shown in (a). Data points correspond to the total fluorescence displayed by the microcolony divided by total microcolony area.

by the high affinity operator sites, so that more atc must be applied in order to have enough LacI that is available for the reporter system.

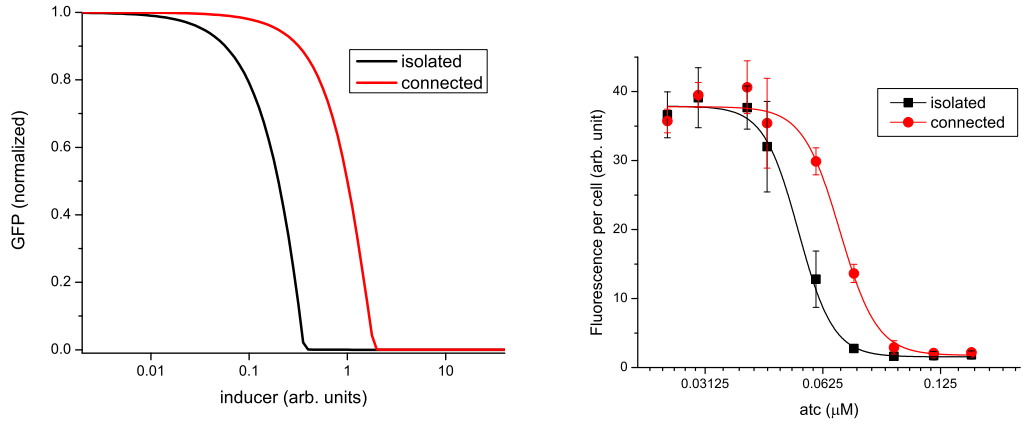

(a) Simulation.

(b) Experiment.

Figure 6: **Retroactivity increases the point of half maximal induction u_{50}.** (a) Normalized simulation results obtained from the model in equations (1). The parameter values for the simulations are given in the SI. (b) Experimental data showing an increase of 30% of the u_{50}. For each data point shown here, three replicates were obtained by growing cells in plate reader. Data was fitted using non-linear regression on a repression-type Hill function model. Error bars denote one standard deviation around average from 3 replicates.

Note that for values of atc exceeding 0.095 μM, the steady state value of the circuit is not appreciably changed by retroactivity while the temporal dynamics is substantially impacted by retroactivity. This illustrates a concrete case in which understanding the extent of modularity requires studying the temporal dynamics.

The increase of the u_{50} can lead to fairly unpredictable results when the module is connected. In fact, based on the response of the module characterized in isolation as seen from the black plot of Figure 6(b), one expects that the maximal change of the output y is obtained by changing the input u about 0.05μM. Hence, one would design the system upstream of the transcription module so that it outputs u in a range about 0.05μM to lead to the maximal change in y. This process is sometimes referred to as input/output matching. Unfortunately, once y connects to downstream clients, a change in the input u about 0.05μM leads to almost no response in y because the true transfer curve is the red one of Figure 6(b). This problem can be overcome by accounting for the increase of u_{50} due to retroactivity when

one performs input/output matching. This is in net contrast with the dynamic effects of retroactivity, which cannot be removed or attenuated by adjusting the input stimulation in the connected system.

2.3 Parametric study of retroactivity effects on a simple model

In order to understand the mechanistic origin of the retroactivity effects observed experimentally and to understand how the parameters of the interconnection control these effects, we consider a simple model suitable for analytical study. For any species X, we denote in italics X its concentration. Consider a transcription component with one input u (a transcription factor or an inducer) and one output Z (a transcription factor), which in turn is used as an input for downstream transcription modules (clients). The model of the isolated system (without the downstream clients) can be written as

$$\frac{dz}{dt} = k(u) - \delta z,$$

in which $z = [Z]/p_T$ with p_T the concentration of the promoter expressing Z. Here, $k(u)$ is the standard Hill function, whose form depends on whether u is an activator or a repressor. Assuming that u is an activator, as it is the case in the experimental system, we have that $k(u) = \alpha\frac{u^n}{1+u^n}$, in which n is the Hill coefficient and u is in units of its dissociation constant. Parameter δ is the decay rate constant modeling dilution and degradation and α is the maximal Z expression rate per promoter. We neglect the mRNA dynamics since they are not significant for our purpose.

When Z is taken as an input by another transcription module, we need to modify the isolated model by including the binding reaction of Z with downstream promoter sites q. Let q_T denote the total amount of promoter sites, k_{on} the association rate constant, and k_{off} the dissociation rate constant. Let c represent the concentration of the complex of Z with

q divided by p_T and let $\lambda = q_T/p_T$ be the ratio between the plasmid copy number of the transcription component and the plasmid copy number of the downstream clients. Then, the connected z dynamics are given by

$$\begin{aligned} \frac{dz}{dt} &= k(u) - \delta z \overbrace{-k_{\text{on}} p_T(\lambda - c)z + k_{\text{off}} c}^{s} \\ \frac{dc}{dt} &= k_{\text{on}} p_T(\lambda - c)z - k_{\text{off}} c - \delta c. \end{aligned} \tag{2}$$

Referring to block diagram of Figure 1, the retroactivity to the output of the transcription module is $s = -k_{\text{on}} p_T(\lambda - c)z + k_{\text{off}} c$, so that the isolated system is obtained by setting $s = 0$ in the above equations.

Steady state effects of retroactivity. To determine the effects that retroactivity s has on the steady state characteristic from u to z, we equate to zero the time derivatives in system (2) and solve both isolated and connected systems for the steady state (see SI for the detailed derivations). In the limit in which the dissociation constant $K_{\text{d}} := k_{\text{off}}/(p_T k_{\text{on}})$ is very small compared to z, we obtain that the main effect of retroactivity is to increase the point of half maximal induction such that

$$u_{50}^{\text{connected}} - u_{50}^{\text{isolated}} \approx \left(\frac{\alpha/\delta + \lambda}{\alpha/\delta - \lambda} \right)^{1/n} - 1.$$

Hence, for $\lambda = 0$ (no downstream clients) there is no change in the u_{50} and as λ increases, the u_{50} of the connected system increases. This increase is more prominent when the maximal z production rate α is smaller.

Dynamic effects of retroactivity. To study the dynamics of z, it is useful to reduce the connected system dynamics to a one dimensional ODE model by exploiting the separation of time scale between protein production and decay and binding/unbinding reactions. Specifi-

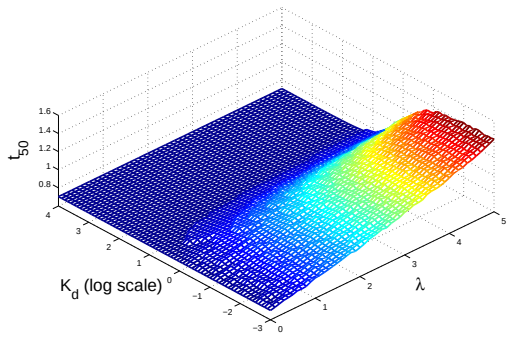

(a) Induction.

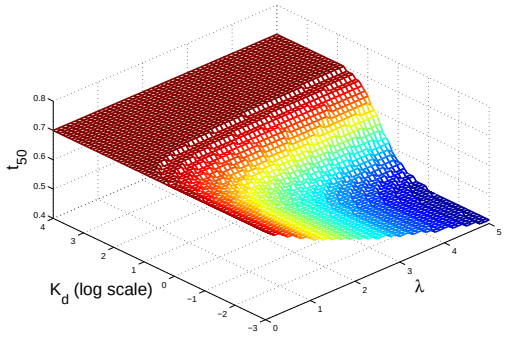

(b) De-induction.

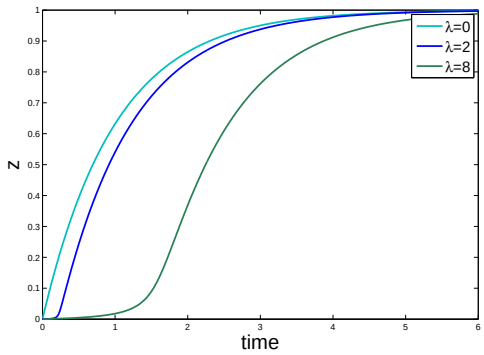

(c) Response for low K_{d} ($K_{\mathrm{d}} = 10^{-4}$).

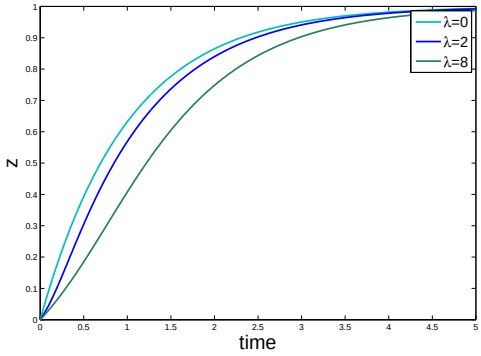

(d) Response for high K_{d} ($K_{\mathrm{d}} = 1$).

Figure 7: **Effect of connection parameters on the t_{50}.** (a) t_{50} response time to a constant input stimulus. As the dissociation constant K_{d} decreases, the response time increases up to a limit after which it saturates. As λ increases, the response time continues to monotonically increase. (b) t_{50} in correspondence to z decaying to zero from an initial value. As the dissociation constant decreases and as the amount of promoter increases, the t_{50} monotonically decreases, that is, the response becomes faster. In these plots, the t_{50} for the isolated system can be found in correspondence to $\lambda = 0$ (no client promoter sites) or $K_{\mathrm{d}} \to \infty$ (Z has no affinity to the promoter sites). (c) shows the effect of increasing λ for low values of K_{d}. (d) shows the effect of increasing λ for high values of K_{d}. In the simulations, we set $k = 10$, $\delta = 1$, and $p_T = 1$.

cally, the dynamics of the connected system can be reduced to (see the SI for details)

$$\frac{dz}{dt} = \left(\frac{1}{1 + dg(z)/dz}\right)(k(u) - \delta z - \delta g(z)), \quad g(z) = \frac{\lambda z}{K_{\mathrm{d}} + z}. \tag{3}$$

This expression becomes close to that of the isolated system when both $g(z)$ and $dg(z)/dz$ are very small. For the induction experiment it is possible to mathematically show that

the response of the connected system is always slower for all values of parameters than the response of the isolated system (see the SI for details), that is, $t_{50,20}^{\text{connected}} > t_{50,20}^{\text{isolated}}$.

Figure 7(a) further shows how the key parameters of the interconnection, that is, λ and K_{d} affect the t_{50}. This response time increases monotonically as λ is increased and as K_{d} decreases. As K_{d} decreases, the t_{50} increases up to a limit, at which the effect of the interconnection becomes a finite time delay (see Figure 7(c)). This time delay monotonically increases with λ and it is given in good approximation by (see the SI for the detailed derivation)

$$\text{time delay} \approx \frac{1}{\delta} \ln \frac{k}{k - \lambda\delta}.$$

When instead K_{d} is higher, some of the z that is produced is free to take place in other reactions even before c reaches its quasi-steady state value. Hence, the effect of the connection is to decrease the effective rate of production of z. Specifically, the effective initial rate of production of z becomes equal to $k(u)/(1 + \lambda/K_{\text{d}})$ (see Figure 7(d)).

For the de-induction experiment, it is possible to mathematically show that the response of the connected system is always faster for all values of parameters than the response of the isolated system (see the SI for details), that is, $t_{50,20}^{\text{isolated}} > t_{50,20}^{\text{connected}}$. Figure 7(b) shows how the key parameters of the interconnection, that is, λ and K_{d} affect the t_{50}. This response time decreases monotonically as λ is increased and as K_{d} decreases. In the limit in which K_{d} is very small, the t_{50} is given by

$$t_{50} \approx \frac{1}{\delta} \ln \left(\frac{\alpha/\delta + \lambda}{\alpha/(2\delta) + \lambda} \right),$$

which decreases monotonically when λ increases.

When the transcription component is taken as an input by $m > 1$ downstream clients, as it occurs in the experimental system, each of which with λ_i relative amount of downstream binding sites with dissociation constant $K_{d,i}$, we obtain the reduced model for the connected

system given by

$$\frac{dz}{dt} = \left(\frac{1}{1+\sum_i^m dg_i(z)/dz}\right)(k(u) - \delta z - \delta \sum_i^m g_i(z)), \quad g_i(z) = \frac{\lambda_i z}{K_{d,i} + z}.$$

It follows that the effects of retroactivity from the downstream clients are qualitatively all the same as each of the downstream clients makes both the multiplying factor $1/(1+\sum_i^m dg_i(z)/dz)$ and the effective production rate smaller.

2.4 Conclusions and Discussion

We have characterized the effects of retroactivity on the temporal dynamics of transcription components in gene circuits *in vivo*. Specifically, we showed that retroactivity from downstream clients leads to a sign-sensitive delay, in which the connected system responds slower to induction but faster to de-induction when compared to the isolated system. Sign-sensitive delays are a common temporal dynamic pattern in the response of microorganisms to changes in environmental conditions and have a number of functions, including noise filtering.[1] A known mechanism to obtain sign-sensitive delays is coherent feedforward loops.[6] Our results show that another and much simpler mechanism to realize a sign-sensitive delay is retroactivity. Indeed, through the addition of DNA binding sites, we can precisely control the speed of response of a transcription circuit to its input stimuli, without changing the structure of the circuit itself. Our formulas of the expected delays and anticipation provide a tool to systematically design the DNA binding sites to obtain the desired dynamic response. This study also reveals that a new, more subtle, role for the large number of inactive promoter sites on the chromosome capable of binding proteins[23] is that of tuning the temporal dynamics of gene transcription.

We also provide a concrete tool that can be used to predict the effects of the composing synthetic biology modules when modularity fails due to retroactivity on a transcription in-

terconnection. From knowledge of the dissociation constant of the transcription factor with respect to its promoter and the relative amount of promoter sites, one can precisely characterize the impact of the interconnection on the behavior of the system. As an example, consider the way synthetic gene circuits are usually characterized. The output, a transcription factor, is measured by employing reporter genes regulated by that transcription factor. These reporters are often placed in high copy number plasmids to obtain a sufficiently high measurement range. As demonstrated in this work, this approach changes the behavior of the circuit one is trying to characterize. However, our results provide a way to explicitly account for the effect of the reporter system in this measurement assay, by adding the provided retroactivity expressions to the model used in the prediction of the circuit behavior.

The quantitative retroactivity models allow evaluation of how particular design choices affect the retroactivity generated by synthetic biology modules. From the mathematical expressions, one can see that placing a downstream circuit in the chromosome or in a very low copy number plasmid, instead of employing a high copy number plasmid, one can dramatically decrease the effect of retroactivity. The same result can be obtained by picking a promoter with lower affinity to the transcription factor. Of course, these choices must be balanced by other design specifications. For example, while a reporter in the genome decreases the impact of retroactivity to the circuit being measured, it may also reduce the signal to a level in which it is highly affected by noise. With a more careful analysis, it may be even possible to understand how complex changes, such as temperature variation, impact retroactivity. In order to do so, it is necessary to understand the exact contribution of these changes to the key parameters in the model: expression and decay rate of the transcription factor, dissociation constant between transcription factor and its binding site and relative ratio of downstream DNA to upstream system DNA. As an example, if we move the assays presented in this paper from 30°C to 37°C, we know that the ratio λ will increase,[26] which will increase retroactivity. This increase in temperature could also lead to a faster decay

rate, due to higher doubling rate and stronger protease activity,[27] which further increases the effect of retroactivity as shown in mathematical expressions given in the Supplementary Information.

A phenomenon related to, but different from, retroactivity occurs when two modules share a resource. If competition for the resource arises between the modules, an indirect connection between them appears,[18,28,29] breaking thus the modularity. However, retroactivity is not a consequence of an unknown indirect connection linking unrelated modules, but the back-effect from the interconnection itself. This subtle difference is important when engineering a solution to these problems. For resource competition problems, a desirable solution is to decouple the modules by employing orthogonal resources or by increasing their availability. For retroactivity, the solution is to enforce unidirectionality of the communication path[24] while preserving the interconnection. One approach to guarantee this is by employing insulation devices,[12] systems that use feedback control and other mechanisms[22,24] to make a system insensitive to potentially high retroactivity, similar to what operational amplifiers do in electronics.

The core mechanism that generates retroactivity in biomolecular circuits is the reversible association between biomolecules. Hence, experimental studies analyzing the impact of protein sequestration by other proteins[30] or by DNA sites[31] on the dose response curve of a system are related to our work. These studies focus only on the steady-state characteristic of circuits and do not provide information on the dynamic response, which is the focus of our work. Furthermore, these studies employ a titrating element (DNA, for example) at concentrations that are several orders of magnitude larger than what is observed in natural or synthetic circuits assembled on plasmids. Our experiments, by contrast, use the same amounts of downstream clients as they would be observed in any synthetic circuit. As a consequence, the ultrasensitivity observed in previous studies,[31] was not observed with the smaller number of binding sites used in our work. However, with the smaller number of

binding sites we have used, dramatic changes on dynamic behavior were observed. This suggests that synthetic circuits built on plasmids will face significant effects of retroactivity on the temporal dynamics while more rarely they will face effects on the steady state.

3 Materials and Methods

3.1 Plasmid construction

The circuit plasmid contains three genes. The genes Plac-gfp-lva, Ptet-lacI-lva and Pconst-tetR-lva were built from parts obtained from either the Registry of Biological Parts or amplified from the *E. coli* K-12 genome. The parts were then sequentially inserted into a pACYC184 backbone in a manner that preserved the chloramphenicol resistance but disrupted the tetracycline resistance gene. The client plasmid employed is a pUC18 plasmid in which the entire lacZα was substituted by a LacI symmetric operator site. The control plasmid is a pUC18 plasmid in which the lacZα was simply removed. In both plasmids, the *bla* gene which confers resistance to ampicilin was preserved. Both plasmids were obtained as a courtesy from Prof. Alexander J. Ninfa Lab at University of Michigan, Ann Arbor.

3.2 Strain and Growth Conditions

In these experiments, we used KL-323 strain[32] obtained from the *E. coli* Genetic Stock Center at Yale University. This strain was chosen for its mutation in the LacI gene, which could potentially interfere with the circuit, as well as for its lack of DNA repair genes, which gives appropriate stability to our constructs. The KL-323 strain has an ochre mutation of the lacZ gene, and therefore it has one copy of the lac promoter, identical to the one regulating the GFP-LVA expression in the circuit. The effect of these additional binding sites in the chromosome is negligible since the relative ratio of this chromosome copy number

to circuit plasmid copy number was measured to be smaller than 1:20, while the ratio of the client plasmid is higher than 2:1, 40 times larger. The strains were made competent and subsequently transformed by employing the standard chemical protocol. The media used in the experiment is the M9 media supplemented with 0.4% glucose, 0.2% casamino acids, 40mg/l tryptophan, 100μg/ml ampicilin, and 34μg/ml chloramphenicol. Cells were inoculated into fresh media from plate or freezer stocks, and incubated at 30°C until mid-log phase (spectrophotometry reading of 0.15 at 600nm with 1cm pathlength). At that point the cells were quickly washed and diluted 7/8-fold. Care was taken to preserve the cells in log phase. These diluted cultures were then placed in a plate reader/incubator (Synergy MX) at 30°C and mild agitation in all experiments. The doubling time under these conditions was of approximately 100-150min, with no significant difference between isolated and connected systems. In longer experiments, cells were kept in mid-log phase via dilutions. No impact on the growth rate was observed due to dilutions, addition or removal of atc (see SI).

3.3 Steady state and dynamic experiments in plate reader

For the steady-state experiments, cells were kept in the plate reader for one generation at which point different levels of atc were added to the individual wells. Cells reached steady state after approximately one generation. The steady-state level was preserved for at least another generation, at which point the cells moved into a late log phase. For the induction experiments, cells grew two generations at which point cells were induced. Data points were automatically acquired by the plate reader every 10 minutes. For the wash experiments, cells were induced with .15uM atc. After 4 generations (400 minutes), the inducer was removed by pelleting and resuspension of the cells in fresh media.

3.4 Dynamic experiments in microscope

For these experiments, cells were immobilized in a 2% agarose pad containing the M9 salts, 0.4% glucose, 0.2% casamino acids, 40mg/l tryptophan, 100μg/ml ampicilin, and 34μg/ml chloramphenicol. To prepare the pad, we added 70μl of the molten preparation to a single channel of a CoverWell perfusion chamber (Grace Bio-Labs, #622503) with sealed inlet and outlet pores. Ten microliters overnight cells prepared as described above were placed on top of the pad, which was sealed with clean coverglass. This setup was placed on a stage-heater in order to provide an internal chamber temperature of around 30°C. Stable steady-state fluorescence was observed for cells after around 3-4h of incubation in the microscope setup.

For induction assays, we prepared a pad similar to the one described above, but with additional 0.125 μM atc. Cells from the initial pad displaying steady-state fluorescence were transferred to the new pad by keeping them in contact for around 15s. The new agarose pad was sealed with new cover glass and the setup was placed in the microscope for around 5-6h until all the cells showed absence of fluorescence. For de-induction, we prepared a pad as the one described above, with no atc. Cells from the induction pad were transferred to the new pad in the same way described above. The agarose pad was then sealed with a new cover glass and the setup was placed in the microscope.

To quantify these experiments, individual cells were manually segmented from the phase image, using MicrobeTracker.[33] Cells belonging to the same microcolony were then quantified together. For each microcolony, the total fluorescence was divided by the total area of the cells in the colony.

3.5 Quantitation of plasmid copy number

In order to obtain the ratio between the amounts of the pUC18-based client plasmid and the pACYC184-based circuit plasmid we quantified the amount of DNA extracted from sam-

ples in experimental conditions (exponential growth at 30°C). Plasmid DNA was extracted by employing a commercial mini-prep kit as in.[34] Then, plasmids were linearized by digestion with EcoRI-HF (NEB) to prevent trapping[35] and quantified employing densitometric analysis.[35,36]

For the pACYC184-based circuit plasmid, the copy number per cell obtained was 32 in the isolated system and 22 in the connected system. The pUC18-based control plasmid presented a copy number of 72 while the client plasmid presented 62 plasmids per cell. Assuming an average of 1.5 genomes per cell, the values obtained are consistent with the value of 30 (30°C) - 70 (37°C) copies per genome of pUC18[26] and 18 copies of pACYC184 per genome.[37] The ratio of control to circuit plasmids was 2.2 in the isolated system and the ratio of client to circuit plasmids was 2.8 for the connected system. Hence, the value of λ is between 2 and 3.

4 Acknowledgments

The authors would like to thank Prof. Alexander J. Ninfa at University of Michigan for having provided plasmids and for his suggestions on the circuit construction and experiments. This work was supported by AFOSR Grant # FA9550-10-1-02.

References

[1] Yosef, N.; Regev, A. *Cell* **2011**, *144*, 886–896.

[2] Kuchina, A.; Espinar, L.; Çağatay, T.; Balbin, A. O.; Zhang, F.; Alvarado, A.; Garcia-Ojalvo, J.; Süel, G. M. *Molecular Systems Biology* **2011**, *7*.

[3] Atkinson, M. R.; Savageau, M. A.; Meyers, J. T.; Ninfa, A. J. *Cell* **2003**, 597–607.

[4] Elowitz, M. B.; Leibler, S. *Nature* **2000**, 339–342.

[5] Stricker, J.; Cookson, S.; Bennett, M. R.; Mather, W. H.; Tsimring, L. S.; Hasty, J. *Nature* **2008**, *456*, 516–519.

[6] Bleris, L.; Xie, Z.; Glass, D.; Adadey, A.; Sontag, E.; Benenson, Y. *Molecular Systems Biology* **2011**, *7*.

[7] Alexander, R. P.; Kim, P. M.; Emonet, T.; Gerstein, M. B. *Science Signaling* **2009**, *2*, 1–4.

[8] Kirschner, M. W.; Gerhart, J. C. *The Plausibility of Life: Resolving Darwin's Dilemma*; Yale University Press, 2005.

[9] Lauffenburger, D. A. *Proc. Natl. Acad. Sci. USA* **2000**, *97*, 5031–5033.

[10] Hartwell, L.; Hopfield, J.; Leibler, S.; Murray, A. *Nature* **1999**, *402*, 47–52.

[11] Alon, U. *An introduction to systems biology. Design principles of biological circuits*; Chapman-Hall, 2007.

[12] Del Vecchio, D.; Ninfa, A. J.; Sontag, E. D. *Mol. Sys. Biol.* **2008**, *4:161*.

[13] Saez-Rodriguez, J.; Kremling, A.; Gilles, E. *Computers and Chemical Engineering* **2005**, *29*, 619–629.

[14] Sauro, H. M. *Mol. Sys. Biol.* **2008**, *4*.

[15] Kim, K. H.; Sauro, H. M. *J. of Biological Engineering* **2010**, *4*.

[16] Jayanthi, S.; Del Vecchio, D. *PLoS ONE* **2012**, *7*.

[17] Cardinale, S.; Arkin, A. P. *Biotechnology J.* **2012**, *7*.

[18] Kim, Y.; Coppey, M.; Grossman, R.; Ajuria, L.; Jiménez, G.; Paroush, Z.; Shvartsman, S. Y. *Curr. Biol.* **2010**, *20*, 446–451.

[19] Kim, Y.; Paroush, Z.; Nairz, K.; Hafen, E.; Jiménez, G.; Shvartsman, S. Y. *Mol. Sys. Biol.* **2011**, *7*, 467.

[20] Ventura, A. C.; Jiang, P.; Van Wassenhove, L.; Del Vecchio, D.; Merajver, S. D.; Ninfa, A. J. *Proc. Natl. Acad. Sci. USA* **2010**, *107*, 10032–10037.

[21] Jiang, P.; Ventura, A. C.; Merajver, S. D.; Sontag, E. D.; Ninfa, A. J.; Del Vecchio, D. *Science Signaling* **2011**, *4*, ra67.

[22] Franco, E.; Friedrichs, E.; Kim, J.; Jungmann, R.; Murray, R.; Winfree, E.; Simmel, F. C. *Proc. Nat. Acad. Sci. USA* **2011**,

[23] Burger, A.; Walczak, A. M.; Wolynes, P. G. *Proc. Nat. Acad. Sci. USA* **2010**, *107*, 40164021.

[24] Jayanthi, S.; Del Vecchio, D. *IEEE Trans. Automatic Control* **2011**, *56*, 748 – 761.

[25] Wong, W.; Tsai, T.; Liao, J. *Molecular Systems Biology* **2007**, *3*.

[26] Lin-Chao, S.; Chen, W. T.; Wong, T. T. *Molecular microbiology* **1992**, *6*, 3385–93.

[27] Purcell, O.; Grierson, C.; Bernardo, M.; Savery, N. *Journal of Biological Engineering* **2012**, *6*, 10.

[28] Cookson, N.; Mather, W.; Danino, T.; Mondragon-Palomino, O.; Williams, R.; Tsimiring, L.; Hasty, J. *Molecular Systems Biology* **2011**, *7*.

[29] Chu, D.; Barnes, D.; von der Haar, H. *Nucleic Acids Research 39*, 6705–6714.

[30] Buchler, C. P.; Louis, M. *J. Mol, Biol.* **2008**, *384*, 1106–1119.

[31] Lee, T.-H.; Maheshri, N. *Molecular systems biology* **2012**, *8*, 576.

[32] Birge, E. A.; Low, K. B. *Journal of Molecular Biology* **1974**, *83*, 447–457.

[33] Sliusarenko, O.; Heinritz, J.; Emonet, T.; Jacobs-Wagner, C. *Molecular Microbiology* **2011**, *80*.

[34] Schmidt, T.; Friehs, K.; Flaschel, E. *Journal of Biotechnology* **1996**, *49*, 219–229.

[35] Projan, S. J.; Carleton, S.; Novick, R. *Plasmid* **1983**, *9*, 182–190.

[36] Pushnova, E.; Geier, M.; Zhu, Y. S. *Analytical biochemistry* **2000**, *284*, 70–6.

[37] Chang, A. C. Y.; Cohen, S. N. *Journal of Bacteriology* **1978**, *134*, 1141–56.